Applied Energy 102 (2013) 1458–1463

Contents lists available at SciVerse ScienceDirect

Applied Energy

journal homepage: www.elsevier.com/locate/apenergy

Analysis and modeling of effective temperature differences and electrical parameters of thermoelectric generators

Shiho Kim *

School of Integrated Technology, Yonsei Institute of Convergence Technology, Yonsei University, Songdo, Inchen 406-840, Republic of Korea

ARTICLE INFO

Article history:
Received 16 March 2012
Received in revised form 15 August 2012
Accepted 3 September 2012
Available online 6 October 2012

Keywords:
Thermoelectric generator (TEG)
Seebeck coefficients
Thermal resistance
Load current dependence
Power generation efficiency

ABSTRACT

We have derived an analytic model describing the interior temperature difference as a function of the load current of a thermoelectric generator (TEG); we have also proposed a method to extract the intrinsic and extrinsic Seebeck coefficients and resistances of TEG using experimental current–voltage curves. The decrement of internal temperature difference is almost linearly depending on load current of the TEG. From the experimental results, using a thermoelectric (TE) module with a thermal conductance of 3.52 W/K and a parasitic thermal conductance of 50 W/K, the effective internal electrical resistance was increased by approximately 5%, but the effective Seebeck coefficient was attenuated by approximately 13%, as compared to the intrinsic parameters. The relationship between the output power reduction factor and limited thermal conductance of TEG packaging was also derived. Approximately 25% of the maximum output power is lost because of the parasitic thermal resistance of the TE module used in the experiment.

1. Introduction

The recycling of waste heat to electrical energy using a thermoelectric generator (TEG) has recently attracted attention in areas where a considerable amount of energy is wasted, such as vehicular applications [1–8]. The TEG is a solid-state energy converter that generates electric power from the temperature difference between its two sides. The internal temperature difference and its dependence on the load current have not been characterized in analytic models [7,8]. The analysis and modeling of the effective temperature difference and electrical properties of the TEG are very important issues in the design of an optimum waste heat recovery system [9]. The prior arts of one-dimensional models can be applied to the study of internal temperature of TEG [10–13]. However, as long as the author knows, an extraction method of model parameters of thermoelectric generator while load current is flowing has not been reported.

In a thermoelectric (TE) module, p-type and n-type thermoelectric pellets sandwiched between ceramic plates are electrically connected in series with a Cu film, as shown in Fig. 1 [10–16]. The effective thermal resistance of the ceramic plate and Cu interconnection layer on both sides of the TE module (θ_H and θ_C) and the thermal resistance of the pellets (θ_m) are connected in series and form a thermal resistance network [3,17,18]. Generally, a TE module is a symmetric structure, designed to have an identical thermal resistance between both hot or cold plates and pellets. The thermal and electrical characteristics of the TEG are represented by the SPICE equivalent model shown in Fig. 2 [12,14–16]. Thermal resistances θ_H or θ_C include parasitic thermal resistance caused by the ceramic plate, Cu layer, and thermal interface material (TIM), and θ_m is the effective thermal resistance formed by a parallel combination of all of the pellets.

TEG can be modeled as a Thevenin voltage source proportional to the Seebeck coefficient with an intrinsic temperature difference between its hot and cold sides, $\alpha_m(T_e - T_a)$, and an intrinsic resistance of R_m, as shown in Fig. 2b [14–16]. The external generated voltage–current relationship is modeled as a Thevenin voltage source V_S proportional to the effective Seebeck coefficient, with a temperature difference between the hot and cold plates, $\alpha_{TEG}(T_H - T_C)$, and an effective resistance of R_{TEG}, as shown in Fig. 2c. The generated output voltage–current relationship is represented by [12,14–16],

$$V = \alpha_{TEG}(T_H - T_C) - R_{TEG}I = \alpha_{TEG}\Delta T - R_{TEG}I. \quad (1)$$

In conventional analysis, the effective Seebeck coefficient (α_{TEG}) is extracted from the measured open circuit voltage divided by the external temperature difference ($T_H - T_C$), and R_{TEG} is extracted from the slope of the I–V curve. If the thermal resistance of the ceramic plates and Cu interconnect is negligible, the temperature of the pellets is identical to the external temperature, but in the TE module, the internal temperature difference of the pellets ($T_e - T_a$) is lower than the external temperature difference ($T_H - T_C$). Because of the parasitic thermal resistance, the temperature difference diminished even under the open circuit condition at the output node of the TEG [17,18].

* Tel.: +82 32 749 3486; fax: +82 32 818 5801.
E-mail address: shiho@yonsei.ac.kr

0306-2619/$ - see front matter © 2012 Elsevier Ltd. All rights reserved.
http://dx.doi.org/10.1016/j.apenergy.2012.09.006

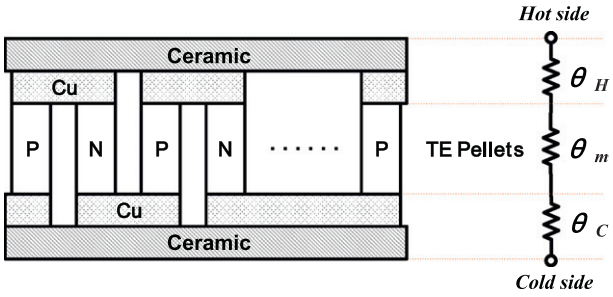

Fig. 1. Structure and thermal resistor network of thermoelectric module.

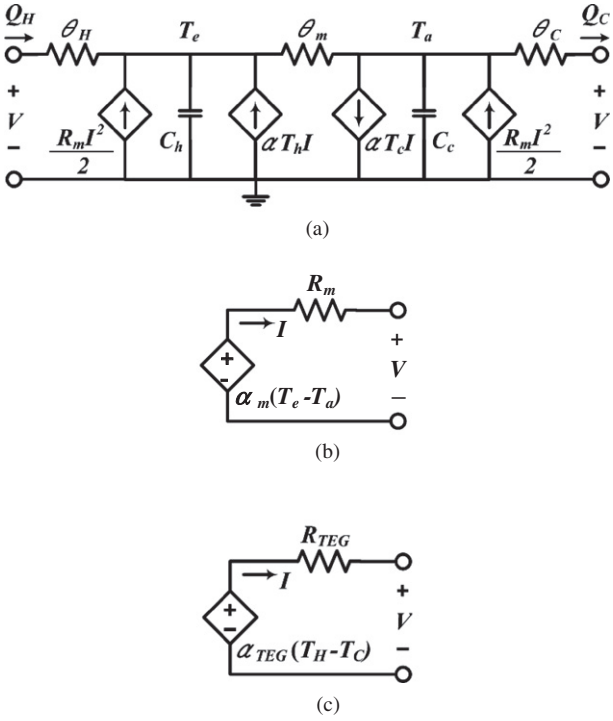

Fig. 2. Electro-thermo equivalent circuit model of TEG. (a) Electric circuit model of thermal behavior, (b) Equivalent source model of TEG with internal temperature difference and (c) Thevenin equivalent source model of TEG with external temperature difference.

It is quite difficult to measure the internal temperature difference between the ends of the pellets while the load current is flowing. Under the condition of a nonzero load current, the internal temperature difference drops, even though the external temperature remains constant. In prior works [17,18], the actual internal temperature difference is calculated by including the parasitic thermal resistance of the TE module under the open circuit condition, and the effective Seebeck coefficient was obtained from the experimental results. However, while the load current is flowing, the internal temperature difference of the TEG drops, which diminishes its power generation efficiency [9]. There have been no prior reports regarding the analytic modeling of the internal temperature difference as a function of the load current or on the influence of the accuracy of the extracted electrical parameters and power generation efficiency.

In this paper, we derive an equation describing the interior temperature difference as a function of the output load current of the TEG and propose a method to extract the effective Seebeck coefficient and electrical resistance of the TEG. Theoretical analysis and parameter extraction methods from the measured data and validation of the approach using SPICE circuit simulation results will be explained in the following sections.

2. Modeling a thermoelectric generator

The rate of supply heat Q_H and removal heat Q_C can be estimated at the hot and cold junction respectively. The heat flow equations of each side of the hot and cold plates are [11–16],

$$Q_H = k_m(T_e - T_a) + \alpha_m I T_e - \frac{I^2 R_m}{2} = k_c(T_H - T_e), \tag{2}$$

$$Q_C = k_m(T_e - T_a) + \alpha_m I T_a + \frac{I^2 R_m}{2} = k_c(T_a - T_C). \tag{3}$$

Here, $(T_e - T_a)$ is the temperature difference of the internal plate of the p- and n-type pellets, and $(T_H - T_C)$ is the temperature difference of the external plate of the TEG. k_c and k_m are the effective thermal conductances of the parasitic components and pellets, respectively, and are the inverse values of thermal resistances θ_C and θ_m, respectively.

The device parameters of TEG linearly depend on area (A), length (L) and the number of pellets (N) [13]. These parameters can be calculated as

$$k_m = \kappa\frac{2NA}{L},\ k_c = \kappa_{(Cu+Ceramic)}\frac{2NA}{L}, R_m = \rho\frac{2NL}{A},\ \text{and } \alpha_m = (2N)s, \tag{4}$$

where s, κ and ρ are the Seebeck coefficient, thermal conductivity and electrical resistivity of the pellets, respectively. $\kappa_{(Cu+Ceramic)}$ is effective thermal conductivity of parasitic components composed of the ceramic plate and Cu interconnects.

We assume a symmetrical structure for the hot and cold plates, so the parasitic thermal conductance of the ceramics and Cu plates are equivalent for the hot and cold plates of the TEG.

By subtracting Eq. (3) from Eq. (2),

$$\alpha_m I(T_e - T_a) - I^2 R_m = k_c(T_H + T_C) - k_c(T_e + T_a). \tag{5}$$

By adding Eq. (2) and (3),

$$2k_m(T_e - T_a) + 2\alpha_m I(T_e + T_a) = k_c(T_H - T_C) - k_c(T_e - T_a), \tag{6}$$

α_m and R_m are the intrinsic Seebeck coefficient and electrical resistance, respectively, of the TEG used to model the electrical characteristics of the TEG.

From Eqs. (5) and (6), we obtain an expression for the temperature difference between the internal hot and cold plates of the TEG (ΔT_{Int}),

$$(T_e - T_a) = \frac{k_c}{2k_m k_c + k_c^2 - \alpha_m^2 I^2}\left(k_c(T_H - T_C) - \frac{\alpha_m R_m I^3}{k_c} - \alpha_m I(T_H + T_C)\right) = \Delta T_{Int}. \tag{7}$$

The Eq. (7) is obtained from the heat flow equations, Eqs. (2) and (3) at hot and cold plate, respectively. Whereas, we assume that the external temperature difference between hot and cold plate, $(T_H - T_C)$, is kept constant during operation. The Eq. (7) indicates that there are three terms influencing the internal temperature difference. The first factor is the voltage divide ratio by thermal resistive network. The second and third terms are representing wattage caused by Joule heating, and wattage due to Peltier effect respectively, while load current is flowing.

When the load current is zero, we obtain ΔT_{Int} under the open circuit condition.

$$\Delta T_{Int}|_{I\to 0} = \Delta T_{i0} = \frac{k_c(T_H - T_C)}{2k_m + k_c}. \tag{8}$$

This expression is the same as the internal temperature difference calculated using the thermal resistor network of a single TE couple [17,18].

By differentiating ΔT_{Int} with respect to load current I, we obtain the slope of the change of the temperature difference, $\partial(\Delta T_{Int})/\partial I$, as follows:

$$\frac{\partial(\Delta T_{Int})}{\partial I} \cong -\frac{\alpha_m(T_H + T_C)}{2k_m + k_c}. \tag{9}$$

The derivation of Eq. (9) is explained in Appendix A. The physical meaning of Eq. (9) is that internal temperature difference of the TEG can be approximated by a linear function of load current, and Peltier effect is the major factor of internal temperature drop caused by the current flowing through a TEG. The slope of change, $\partial(\Delta T_{Int})/\partial I$, is dependent with size of TE module, because the value of TE module parameters, k_m, k_c and α_m, are linear function of area, length and the number of pellets [13].

Because the slope of the change of the temperature difference is almost independent of the load current, as shown in Eq. (9), we can model the linear dependence of the interior temperature difference on the load current.

$$\Delta T_{Int} \cong \frac{k_c(T_H - T_C)}{2k_m + k_c} - \frac{\alpha_m(T_H + T_C)I}{2k_m + k_c}. \tag{10}$$

The first term in Eq. (9) is the temperature attenuation due to the thermal resistor network comprising k_c and k_m, and the second term is the temperature drop caused by the Peltier effect. From the electrical model of the TEG, we obtain the relationship between the terminal voltage and load current, as follows:

$$V = \alpha_m \Delta T_{Int} - R_m I \cong \alpha_m \Delta T_{i0} - \left(R_m + \frac{\alpha_m^2(T_H + T_C)}{2k_m + k_c}\right) I$$
$$= \frac{\alpha_m k_c}{2k_m + k_c}(T_H - T_C) - R_{TEG} I. \tag{11}$$

where R_m is the internal resistance and R_{TEG} is the effective terminal electrical resistance of the thermoelectric generator.

From Eqs. (1) and (11), we can determine the relationship between the intrinsic and extrinsic parameters of the TEG,

$$\alpha_{TEG} = \left(\frac{k_c}{2k_m + k_c}\alpha_m\right), \tag{12}$$

$$\text{and } R_{TEG} = \left(R_m + \frac{\alpha_m^2(T_H + T_C)}{2k_m + k_c}\right). \tag{13}$$

3. Extraction of TEG parameters

A TEG module (TMH400302055, manufactured by Wise Life Technologies) with 199 TE couples was used in the experiment. The geometric features and thermal and electrical parameters of the TE module used in the experiments are listed in the Refs. [3,18]. The calculated thermal conductance (k_m) of all 398 pellets of TMH400302055, including the TIM between the Cu interconnecting layer, is approximately 3.52 W/K, and the thermal conductance of the ceramic plate and Cu interconnects (k_c) is approximately 50.0 W/K.

Fig. 3 shows the experimental curves of the output voltage versus the current, which are fit well to straight lines for several measurement condition of $(T_H - T_C)$, as reported in prior works [1,3,10–17].

We have no direct approach for measuring the interior temperature difference ΔT_{Int} of the TEG during power generation. We therefore propose a procedure for the extraction of the interior temperature difference as well as the electrical parameters using the measured electrical data, as follows:

(1) Extraction of thermal conductance, k_m and k_m.
(2) Calculation of ΔT_{i0} using Eq. (8).

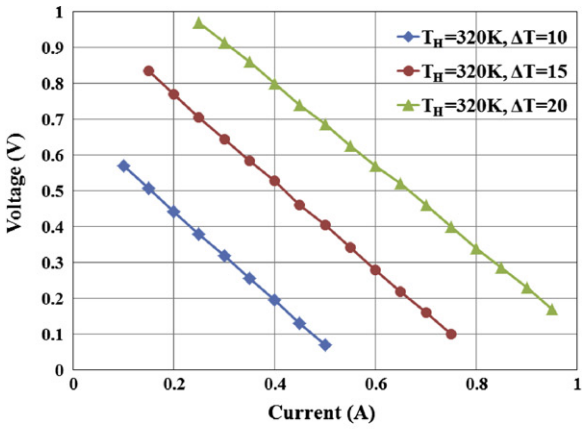

(a)

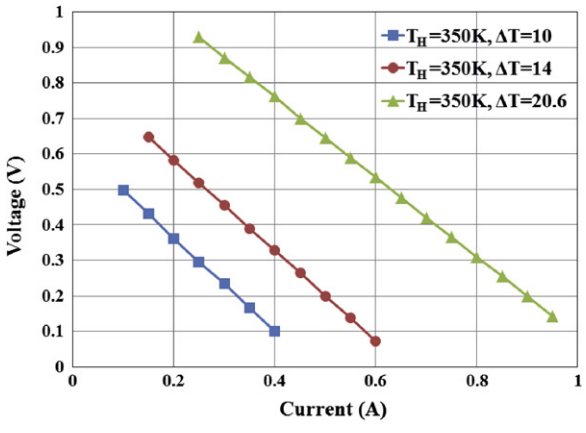

(b)

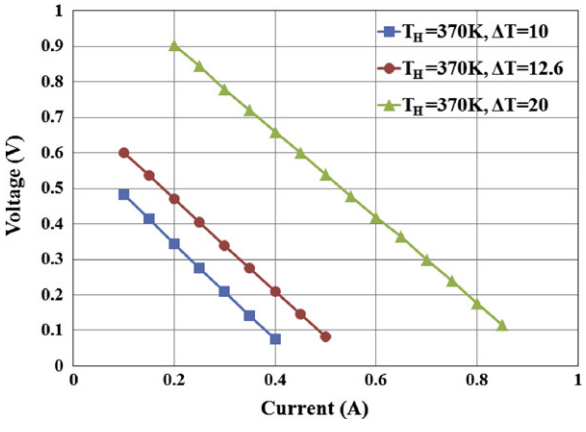

(c)

Fig. 3. Measured voltage-versus-current characteristics of a Bi_2Te_3 thermoelectric module for various hot side temperatures (T_H) and temperature differences ($\Delta T = T_H - T_C$) between hot and cold plates. (a) For T_H = 320 K, (b) for T_H = 350 K, and (c) for T_H = 370 K.

(3) Extraction of α_{TEG} and R_{TEG} from the V-axis intersection (V_{oc}) and slope of the curve, respectively. From the measured I–V curve, $\alpha_{TEG} = V_{oc}/(T_H - T_C)$ and R_{TEG} is the slope of the line of best fit of the measured data.
(4) Calculation of α_m, using Eq. (12)
(5) Calculation of R_m, using Eq. (13)
(6) Calculation of ΔT_{Int}, using Eq. (7) or Eq. (10)

We only need two thermal conductance parameters, k_c and k_m, for the analysis and extraction of the electrical parameters from the measured data.

4. Experimental results and discussions

We calculated the internal temperature difference, Seebeck coefficient, and internal electrical resistance according to the proposed procedure, using the experimental *I–V* curves. The calculated internal temperature difference, as a function of load current using Eqs. (7) and (10), shows a good linear fit. We found the slope of the change of temperature difference ΔT_{Int} with respect to the load current to be approximately −0.88 °C/A, which coincided with the value calculated using Eq. (10), as shown in Fig. 4. The experimental *I–V* curves for hot side temperatures of 330 K and 340 K are not shown in this paper for simplicity, because the trend of the experimental curve was similar. The thermal resistance of the contact material comprising the ceramic plate, Cu interconnect, and solder between the TE pellets and Cu, degrade the performance of the TEG [17,18]. Fig. 5 shows the extracted values of the intrinsic and external Seebeck coefficients as functions of temperature. The external Seebeck coefficient is approximately 87% of the intrinsic one, a degradation ratio that is consistent with the results of prior work using the same type of TEG [17,18].

Fig. 6 shows the extracted electrical resistance obtained from the slopes of the measured *I–V* curves, R_{TEG}, and the calculated internal resistance value, R_m, using Eq. (13). The effective external resistance value is increased by approximately 5% because of a drop in the internal temperature difference in the temperature range 320–370 K in the experiment when k_c is approximately 50 W/K and k_m is approximately 3.52 W/K. Experimental results from Refs. [14–19] shows that temperature dependence of Seebeck coefficient and electrical resistivity of bulk thermoelectric material is nonlinear. The electrical conductivity and Seebeck coefficient are tightly related to the carrier concentration, and carrier mobility caused by various scattering effects which strongly depends on temperature [10,19].

Fig. 7 shows the measured data, the SPICE-simulated data using the equivalent circuit shown in Fig. 2b, and the calculated data from Eq. (10). The calculated and simulated data using the proposed model and extraction procedure coincide quite well with the measured data.

Because the internal electrical resistance of the TEG in the SPICE model includes thermal behavior, it is necessary to use R_m instead of R_{TEG}. R_{TEG} implicitly includes the load current effect on the drop in internal temperature difference. For this reason, in the discrete model that does not consider the cross-coupled action of the electro-thermal behavior, it is necessary to use R_{TEG} as an internal source

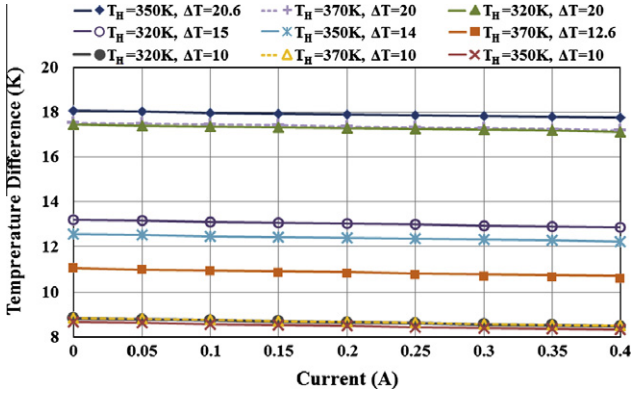

Fig. 4. Calculated internal temperature difference using Eq. (6) (markers) and Eq. (9) (lines).

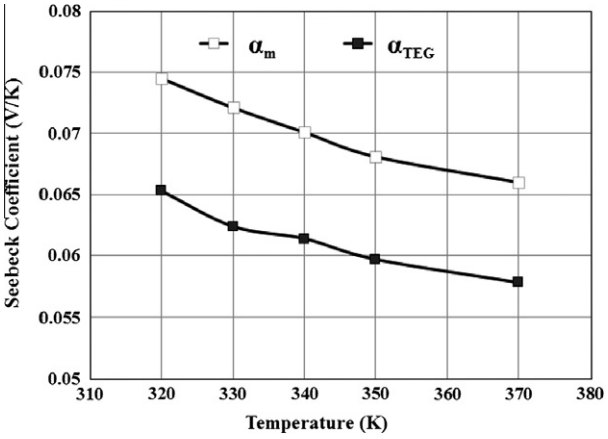

Fig. 5. Extracted Seebeck coefficients from the measured *I–V* curves.

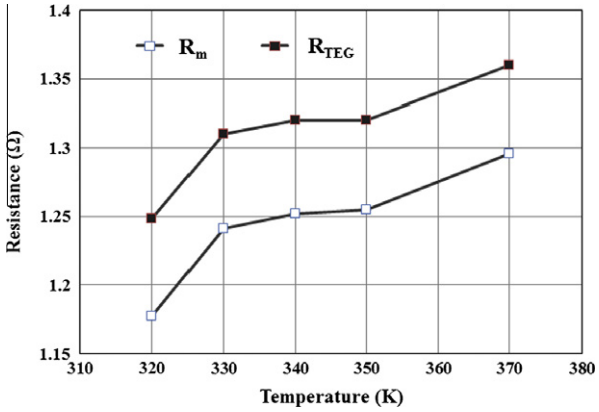

Fig. 6. Extracted electrical resistances from the measured *I–V* curves.

resistance value. It is very hard to specify the limitation of temperature difference that the SPICE model could be applied on TEG modules. For larger temperature difference, we need to extract SPICE parameters for an average temperature of the TE pellet [12–14,16].

The finite value of the thermal conductance between the TE pellets and the contact plate of the heat source causes significant degradation in the output performance of the TEG because of an increase in the internal resistance and attenuation of the effective Seebeck coefficient.

There may be nonlinear effects, in a wide range of temperature difference between hot and cold side, or at high hot temperature operation, due to the temperature dependence of material parameters [11–16,19]. For example, the hot temperature can go from 373 K to 623 K in vehicular applications of TEG [1–8,19,20].

The basic assumption of the approach is that heat flow equations, Eqs. (2) and (3), are valid, and thermal conductance is not changed by load current. In order to apply the proposed procedure in a wide range of temperature difference, we need to re-calculate thermal conductance value of the operating temperature at the initial step of the extraction procedure using datasheets [21]. The main goal of this paper is to derive an analytic model describing the interior temperature difference as a function of the load current. Providing a simple method to extract the intrinsic and extrinsic Seebeck coefficients and resistances of TEG using experimental current–voltage curves is another purpose of the work. The investigation of physical reason of temperature dependence of thermal conductance at high temperature is beyond the scope of this work.

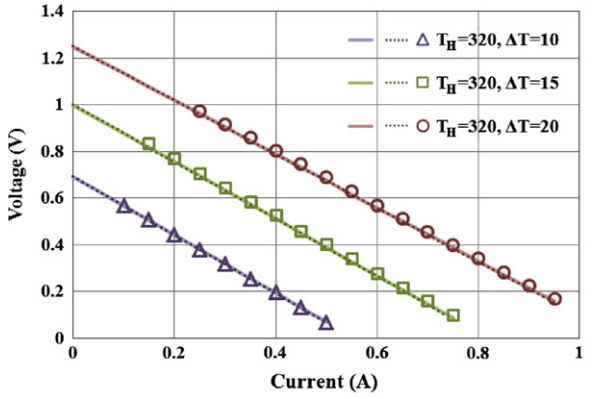

(a)

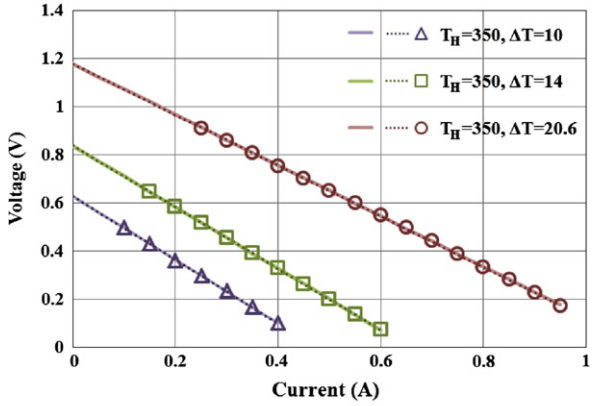

(b)

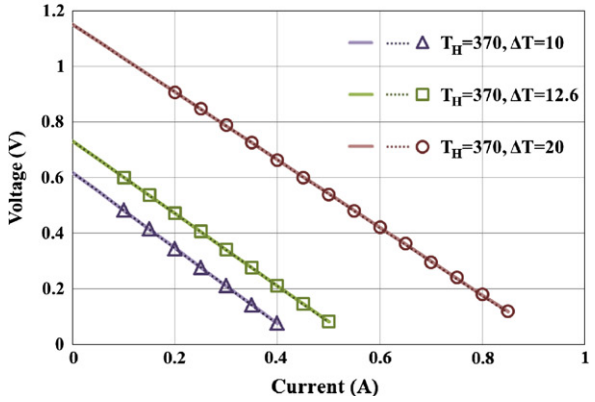

(c)

Fig. 7. Voltage–current curves of measured data (markers), SPICE-simulated (dotted lines) data, and calculated data using Eq. (10) (solid lines). (a) For T_H = 320 K, (b) for T_H = 350 K, and (c) for T_H = 370 K.

Maximum output power is achieved under the load matching condition, when the load resistance is equal to the source resistance of the TEG. Since the *I–V* curve is linear, the maximum output power is [1,22–25]

$$P_{MAX} = \frac{V_{oc}^2}{4R_{TEG}} \tag{14}$$

By substituting the relationship of V_{oc} and R_{TEG} into Eq. (13), we obtain

$$P_{MAX} = \frac{\alpha_m^2 (T_H - T_C)^2}{4R_m} \times \frac{(k_c/k_m)^2}{(2 + k_c/k_m)\{(2 + k_c/k_m) + Z_T/4\}}. \tag{15}$$

Z_T is the figure of merit of the TEG. The derivation procedure for Eq. (14) is described in Appendix B.

In Eq. (14), the theoretical maximum power generated by the TEG is

$$\frac{\alpha_m^2 (T_H - T_C)^2}{4R_m}. \tag{16}$$

Hence, the performance derating factor due to the limited thermal conductance of the plates is

$$\eta_d = \frac{(k_c/k_m)^2}{(2 + k_c/k_m)\{(2 + k_c/k_m) + Z_T/4\}}. \tag{17}$$

For the given values of k_c = 50 W/K and k_m = 3.52 W/K, the output power derating factor, η_d, is approximately 0.75, implying that the output power is reduced by 25% owing to the limited thermal conductance of the packaging and the interconnecting material comprising the ceramic plate and the Cu interconnect layer of the TE module. The derating factor is a function of geometry of a TEG, because the thermal conductances of TEG linearly depend on the area, length, and the number of TE module.

5. Conclusions

We have derived an equation describing the interior temperature difference as a function of the load current of the TEG and have proposed a method to extract the effective Seebeck coefficient and electrical resistance of the TEG using experimental *I–V* curves. The internal temperature difference decreases almost linearly with the load current of the TEG because the wattage due to Peltier effect creates temperature drop across interface materials. From the experimental results using the TE module with a thermal conductance of 3.52 W/K and a parasitic thermal conductance of 50 W/K, the effective internal electrical resistance increased by approximately 5%, but the effective Seebeck coefficient was attenuated by approximately 13%, as compared to the intrinsic parameters. The theoretical relationship of the output power reduction factor caused by internal temperature drops was also derived. Approximately 25% of the maximum output power was lost because of the parasitic thermal resistance of the TE module used in the experiment. Parameter extraction and analysis using the measured data and SPICE-simulated results show that the proposed approach is valid for the modeling and estimation of the performance of a TEG.

Acknowledgments

This work was supported by Yonsei University in 2011. The author thanks Ms. Youngkyo Gim for extracting the experimental data. The SPICE circuit simulator used in this research was supported by IDEC. The Yonsei Institute of Convergence Technology is supported by the Ministry of Knowledge Economy (MKE), under the "IT Consilience Creative Program", supervised by the NIPA (NIPA-271 2010-C1515-1001-0001).

Appendix A

Rewriting Eq. (7), the equation of the internal temperature difference of the TEG is

$$\Delta T_{Int} = \frac{k_c}{2k_m k_c + k_c^2 - \alpha_m^2 I^2}\left(k_c(T_H - T_C) - \frac{\alpha_m R_m I^3}{k_c} - \alpha_m I(T_H + T_C)\right) = \frac{c - dI^3 - eI}{a^2 - b^2 I^2}. \tag{A1}$$

Variables *a*, *b*, *c*, *d*, and *e* in Eq. (A1) are as follows:

Table A1
Typical values of the TE module parameters and coefficients used in the experiment described in this paper.

TEG parameters		Variables in Eqs. (A1)–(A7)			
Parameters	Values	Coefficients	Values	Coefficients	Values
k_c	50	a	2852	bd	4.1×10^{-4}
k_m	3.52	b	4.9×10^{-3}	be	12
α_m	0.07	c	50000	bc	245
R_m	1.2	d	8.5×10^{-2}	ae	7.2×10^{6}
T_H	370	e	2520	ab	14
T_C	350	ad	240	a^2	8.2×10^{6}

$$a = 2k_m k_c + k_c^2, \tag{A2}$$

$$b = \alpha_m^2, \tag{A3}$$

$$c = k_c^2 (T_H - T_C), \tag{A4}$$

$$d = \alpha_m R_m, \tag{A5}$$

$$e = \alpha_m k_c (T_H + T_C). \tag{A6}$$

Differentiating the temperature difference with respect to load current I gives

$$\frac{\partial(\Delta T_{Int})}{\partial I} = \frac{bdI^4 - (3ad + be)I^2 + 2bcI - ae}{bI^4 - 2abI^2 + a^2}. \tag{A7}$$

Because the Seebeck coefficient of TEG, α_m, is relatively very small, the effective value of parameters b, bc, bd, be, and d is negligible compared to the values of ab, ad, or ae.

As an example, the typical values of the TE module parameters and coefficients used in the experiment described in this paper are listed in Table A1.

We can simplify Eq. (A7) as follows:

$$\begin{aligned}\frac{\partial(\Delta T_{Int})}{\partial I} &\cong -\frac{3adI^2 + ae}{-2abI^2 + a^2} = -\frac{3dI^2 + e}{-2bI^2 + a} \cong -\frac{e}{a} \\ &= -\frac{\alpha_m (T_H + T_C)}{2k_m + k_c}.\end{aligned} \tag{A8}$$

Appendix B

By substituting the relationship of the open circuit voltage, V_{oc}, and R_{TEG} into Eq. (14), we obtain

$$\begin{aligned}P_{MAX} &= \frac{\left(\frac{\alpha_m k_c}{2k_m + k_c}(T_H - T_C)\right)^2}{4(R_m + \frac{\alpha_m^2 (T_H + T_C)}{2k_m + k_c})} \\ &= \frac{(\alpha_m (T_H - T_C))^2}{4R_m} \times \frac{(k_c/2k_m + k_c)^2}{1 + \alpha_m^2 (T_H + T_C)/4R_m (2k_m + k_c)} \\ &= \frac{\alpha_m^2 (T_H - T_C)^2}{4R_m} \times \frac{k_c^2}{(2k_m + k_c)\left((2k_m + k_c) + \frac{\alpha_m^2 (T_H + T_C)}{4R_m}\right)}.\end{aligned} \tag{B1}$$

Since figure of merit Z_T is given by [10–16]

$$Z_T = \frac{\alpha_m^2 (T_H + T_C)}{R_m k_m}. \tag{B2}$$

We can rewrite Eq. (B1) as follows:

$$P_{MAX} = \frac{\alpha_m^2 (T_H - T_C)^2}{4R_m} \times \frac{(k_c/k_m)^2}{(2 + k_c/k_m)\{(2 + k_c/k_m) + Z_T/4\}}. \tag{B3}$$

In the case of a small Z_T, $Z_T/4$ is negligible compared to $2 + k_c/k_m$, and hence, P_{MAX} is simplified to

$$P_{MAX} \approx \frac{\alpha_m^2 (T_H - T_C)^2}{4R_m} \times \left(\frac{k_c/k_m}{2 + k_c/k_m}\right)^2. \tag{B4}$$

References

[1] Kim SH, Park S, Kim S, RHI S. A thermoelectric generator using engine coolant for light-duty internal combustion engine-powered vehicles. J Electron Mater 2011;40:812–6.
[2] Hsu CT, Huang GY, Chu H, Yu B, Yao D. Experiments and simulations on low-temperature waste heat harvesting system by thermoelectric power generators. Appl Energy 2011;88:1291–7.
[3] Hsiao Y, Chang WC, Chen SL. A mathematic model of thermoelectric module with applications on waste heat recovery from automobile engine. Energy 2010:1447–54.
[4] Liang G, Zhou J, Huang X. Analytical model of parallel thermoelectric generator. Appl Energy 2011;88:5193–9.
[5] Gou Xiaolong, Xiao Heng, Yang Suwen. Modeling, experimental study and optimization on low-temperature waste heat thermoelectric generator system. Appl Energy 2010;87:3131–6.
[6] Suter C, Jovanovic ZR, Steinfeld A. A 1 kWe thermoelectric stack for geothermal power generation-modeling and geometrical optimization. Appl Energy 2012;99:379–85.
[7] Yao DJ, Yeh KJ, Hsu CT, Yu BM, Lee JS. Efficient reuse of waste energy. IEEE Nanatechnol Mag 2009;3:28–33.
[8] Niu X, Yu J, Wang S. Experimental study on low-temperature waste heat thermoelectric generator. J Power Sources 2009;188:621–6.
[9] Spry M. Improving the testing of power generation modules and resulting performance projections. In: Proc int conference on thermoelectrics, Traverse City, USA; 2011.
[10] Hogan TP, Shih T. Modeling and characterization of power generation modules based on bulk materials. CRC thermoelectrics hanbook, macro to nano. CRC Press; 2006 [chapter 12].
[11] Seifert W, Ueltzen M, Müller E. One-dimensional modeling of thermoelectric cooling. Phys Status Solidi (a) 2002;194(277–9).
[12] Mitrani D, Salazar J, Turo A, Garcia MJ, Chavez J. One-dimensional modeling of TE devices considering temperature-dependent parameters using SPICE. Microelectron J 2009;40:1398–405.
[13] Hodes M. On one-dimensional analysis of thermoelectric modules. IEEE Trans Compon Pack Technol 2005;20:218–29.
[14] Charvez J, Ortega J, Salazar J, Turo A, Garcia M. SPICE model of thermoelectric elements including thermal effects. In: Proc IEEE instrumentation and measurement technology conference, Baltimore, USA; 2000.
[15] Mitrani D, Tome A, Salazar J, Turo A, Garcia M, Charvez J. Methodology for extracting thermoelectric module parameters. IEEE Trans Instrum Meas 2005;54:1548–52.
[16] Lineykin S, Ben-Yaakov S. Modeling and analysis thermoelectric modules. IEEE Trans Ind Appl 2007;43:505–12.
[17] Hsu CT, Huang GY, Chu HS, Yu B, Yao DJ. An effective Seebeck coefficient obtained by experimental results of a thermoelectric generator module. Appl Energy 2011;88:5173–9.
[18] Hsu CT, Huang GY, Chu HS, Yu B, Yao DJ. Experiments and simulations on low temperature waste heat harvesting system by thermoelectric power generators. Appl Energy 2011;88:1291–7.
[19] Yamashita Osamu. Effect of temperature dependence of electrical resistivity on the cooling performance of a single thermoelectric element. Appl Energy 2008;85:1002–14.
[20] Han H, Kim Y, Kim S, Um S, Hyun J. Performance measurement and analysis of a thermoelectric power generator. In: IEEE intersociety conference on thermal and thermomechanical phenomena in electronic systems (ITherm), Las Vegas, USA; 2010.
[21] Luo Z. A simple method to estimate the physical characteristics of a thermoelectric cooler from vendor datasheets. Electron Cooling 2008;14:22–7.
[22] Kim R, Lai J, York B, Koran A. Analysis and design of maximum power point tracking scheme for thermoelectric battery energy storage system. IEEE Trans Ind Electron 2009;56:3709–16.
[23] Jensak E, Itsda B. Development of a thermoelectric battery-charger with microcontroller-based maximum power point tracking technique. Appl Energy 2006;83:687–704.
[24] Kim SH, Cho S, Kim N, Baatar N, Kwon J. A digital coreless maximum power point tracking circuit for thermoelectric generators. J Electron Mater 2011;40:867–72.
[25] Carmo JP, Antunes J, Silva M, Ribeiro J, Goncalves L, Correia J. Characterization of thermoelectric generator by measuring the load-dependent behavior. Measurement 2011;44:2194–9.